Korean J. Chem. Eng., **27**(4), 1192-1204 (2010)
DOI: 10.1007/s11814-010-0185-8

Numerical simulation of secondary clarifier with activated sludge and suction lift removal system: Modified Casson model and sludge withdrawing sensitivity analysis

Muhammad Reza Saffarian, Mohammad Hossein Hamedi, and Mehrzad Shams†

Faculty of Mechanical Engineering, K.N.Toosi University of Technology, Pardis St., Mola Sadra St., Vanak Sq., Tehran, Iran
(*Received 27 June 2009 • accepted 18 November 2009*)

Abstract−A computational fluid dynamics model that predicts the sedimentation of activated sludge in a circular secondary clarifier with activated sludge is developed. The axisymmetric single-phase flow is simulated by using a CFD code that has been written with Intel Visual Fortran. First, sludge withdrawing by suction-lift in the near-bottom region of the clarifier is simulated using suction at the bottom of clarifier. The flow and settling processes are simulated using k-ε turbulence model on a two-dimensional and orthogonal grid. A convection–dispersion equation that is extended to incorporate the sedimentation of activated sludge in the field of gravity is used. The computational domain includes the sludge blanket where the viscosity is affected by the rheological behavior of the sludge. Experimental data provided by Weiss et al. show that the relationship between shear stress and shear rate follows the Casson law for the shear rates lower than 50 s^{-1}. Plastic viscosity of activated sludge is not removed from the concentration diffusion, so using regular non-Newtonian models leads to overestimation of blanket height. Modified Casson model is introduced to overcome the blanket height overestimation problem. Results show that the local sludge distribution in the clarifier has excellent agreement with concentration profile measurements of Weiss et al., for different treatment plant loadings. Alternative sludge withdrawing methods include withdrawing from pipes position at the bottom of clarifier and withdrawing by using sink terms in governing equations are used. Results show that the first withdrawing method gives less error comparing to these withdrawing methods.

Key words: Turbulence, Secondary Clarifier, Concentration, Activated Sludge, Modified Casson Model

INTRODUCTION

Secondary clarifiers represent the final stage in the activated sludge wastewater treatment process. They are preceded by the aeration basin, where previously developed biological sludge flocs are brought into contact with the organic material in the wastewater. The first theory about the efficiency of settling tanks was developed by Hazen (1904) for individual particle settling in a uniform flow [1-3]. Anderson (1945) discovered that the flow is far from uniform because of density stratification. The solids-loaded influent has a higher density than the ambient water and, hence, plunges as a density jet to the bottom of the tank; this is the so-called density current [1-3].

Schamber and Larock (1981) introduced the k-ε turbulence into a finite element model and assumed pure water flow and a simplified inlet configuration at the surface to simulate neutral density flow in the settling zone of a rectangular tank [3,4]. Imam et al. (1983) used a finite difference code with the constant eddy viscosity approach but considered also suspension distribution and somewhat more realistic tank geometry with an inlet baffle. They carried out experiments in order to calibrate the value of the eddy viscosity and to verify the numerical results [1,3,4]. Using a finite-volume code, Celik and Rodi (1985) applied the k-ε model to simulate the same experiment of Imam et al. approximating the settling properties of the suspension by a constant settling velocity [4]. Some modeling studies were also made on the influence of buoyancy (DeVantier and Larock, 1987; Adams and Rodi, 1988; Zhou and McCorquodale, 1992) and flocculation (DeVantier and Larock, 1987; Lyn et al., 1992) on the flow and settling in final clarifiers [2-4]. Krebs (1991) examined the influence of sludge removal on buoyancy-affected flow and performed calculations of the flow in a rectangular tank, including continuous flight scraper sludge removal against the main flow direction [4]. Because of convergence difficulties, turbulence could be modeled only by the constant eddy viscosity approach. The first attempt to model the flow in a radial section of a circular tank was due to DeVantier and Larock (1987), who used a finite element method and the k-ε turbulence model [4].

Van Marle and Kranenburg (1994) indicated that if short circuiting is prevented, the density current that appears in the vicinity of the solids blanket is beneficial for the settling tank performance. Krebs et al. (1999) came to similar conclusions; however, when strong density effects prevail, as is usually the case in secondary settling tanks, increased tank depths are recommended [1]. Experiments of Konicek and Burdych (1988) show flocculation in the density current, being beneficial for the solids removal efficiency [1].

Numerical modeling of secondary clarifiers gained an advanced state of development in the past years (Krebs, 1991, 1995; Lyn et al., 1992; Zhou and McCorquodale, 1992; Dahl et al., 1994; Szalai et al., 1994; Holthausen, 1995). Nowadays, it is possible to simulate the internal three-dimensional flow patterns of the clarifier. Corresponding measurements of concentration data are scarce; however, full scale measurements of velocity distributions have been mainly conducted in rectangular secondary settling tanks (Larsen, 1977; Bretscher and Hager, 1990; Bretscher et al., 1992; Baumer et al.,

†To whom correspondence should be addressed.
E-mail: shams@kntu.ac.ir

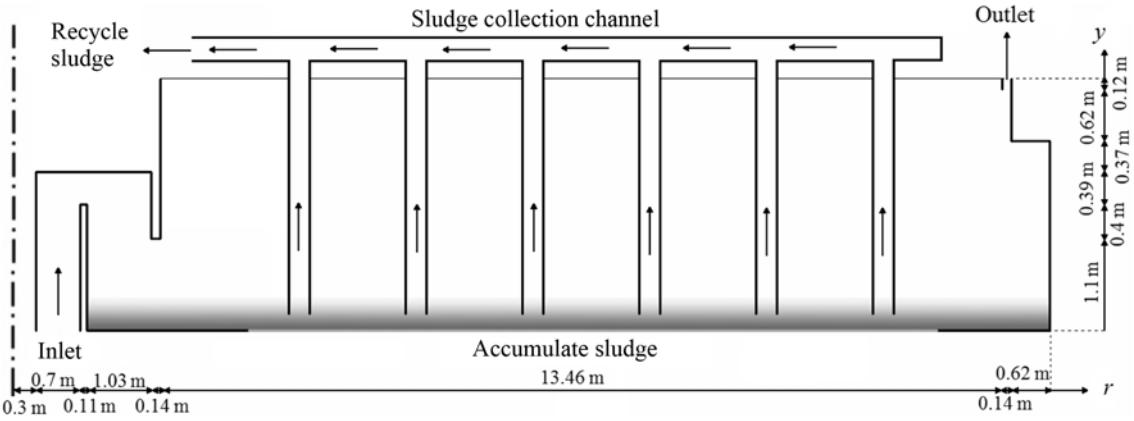

Fig. 1. Geometry of settling tank.

1995; Überl, 1995) [5].

Recently, a rheology function to account for the increased viscosity of highly concentrated sludge mixtures has been used by Lakehal et al. [2], DeClercq [1], McCorquodale et al. [3] and Weiss et al. [6], investigating flow of activated sludge in secondary clarifier.

The present study deals with density-affected flow in circular clarifiers equipped with suction-lift sludge removal systems as shown in Fig. 1. In these clarifier systems, which usually have a flat bottom, the sludge is withdrawn through an array of vertical suction pipes from the near-bottom region [6]. These pipes are situated underneath the slowly rotating clarifier bridge and remove sludge locally underneath the bridge. This study describes a CFD model of the flat-bottom secondary clarifiers at a wastewater treatment plant in the north-west of France, which has been constructed for 122,000 inhabitant-equivalents and that consists of two identical biological treatment lines. Each treatment line consists of one continuously fed aeration basin and two identical secondary clarifiers [6]. The region of the sludge blanket is included in the calculation domain. This approach allows the computation of the sludge blanket height and the concentration profiles within the sludge blanket. The influence of stratification on the turbulence properties is considered by means of sink terms in the equations of turbulent kinetic energy.

MATHEMATICAL MODEL

The flow field is obtained by solving the Reynolds-averaged Navier-Stokes equations in a cylindrical coordinate system. The k-ε model is used for turbulence modeling. The suspended sediment concentration is determined by solving a passive scalar equation, in which the particle settling velocity is introduced. The buoyancy effect is defined as, ρg, where ρ is the local mixture density, and g is the gravitational acceleration. This results from the sediment-induced density differences and is accounted by considering a sink term in the vertical momentum equation. Also, the damping influence of stratification on the production of turbulent kinetic energy is expressed as a sink term appearing in the transport equations of turbulent kinetic energy, k, and its rate of dissipation, ε [2,6]. The system of Reynolds-averaged Navier-Stokes equations for two-dimensional, axisymmetric, unsteady, density-stratified, and turbulent mean flow may be given as [2,6]:

$$\frac{\partial \rho}{\partial t}+\frac{\partial(\rho u)}{\partial r}+\frac{\partial(\rho v)}{\partial y}+\frac{\rho u}{r}=0 \tag{1}$$

$$\frac{\partial(\rho u)}{\partial t}+\frac{1}{r}\frac{\partial(r\rho uu)}{\partial r}+\frac{\partial(\rho uv)}{\partial y}=-\frac{\partial p}{\partial r}+\frac{1}{r}\frac{\partial}{\partial r}\left(r(\mu+\mu_t)\frac{\partial u}{\partial r}\right)+\frac{\partial}{\partial y}\left[(\mu+\mu_t)\frac{\partial u}{\partial y}\right]-\frac{\rho u}{r^2} \tag{2}$$

$$\frac{\partial(\rho v)}{\partial t}+\frac{1}{r}\frac{\partial(r\rho uv)}{\partial r}+\frac{\partial(\rho vv)}{\partial y}=-\frac{\partial p}{\partial y}+\frac{1}{r}\frac{\partial}{\partial r}\left(r(\mu+\mu_t)\frac{\partial v}{\partial r}\right)+\frac{\partial}{\partial y}\left[(\mu+\mu_t)\frac{\partial v}{\partial y}\right]-\rho g \tag{3}$$

In the above equations the origin of the coordinate system is placed on the vertical center line, with the *y*-axis pointing vertically upwards from the bottom boundary. The field equations are given in terms of averaged flow variables, where u and v are the mean velocity components in the r (radial) and y (axial) directions, respectively. Also t is the time, p is the pressure, ρ is the density of the mixture, g is the gravitational acceleration constant, μ is the viscosity of the sludge mixture, and μ_t is the turbulent viscosity. The governing field equations are formulated using the density of mixture.

1. Standard k-ε Turbulence Model

The turbulent viscosity, μ_t, is determined by the turbulent kinetic energy, k, and by the rate of dissipation of turbulence kinetic energy, ε, according to [1-4,6,7]:

$$\mu_t=\rho C_\mu\frac{k^2}{\varepsilon} \tag{4}$$

where C_μ=0.09 is a constant [1-4,6,7]. The semi-empirical model, transport equations for k and ε may be given as [2,6]:

$$\frac{\partial(\rho k)}{\partial t}+\frac{1}{r}\frac{\partial(r\rho uk)}{\partial r}+\frac{\partial(\rho vk)}{\partial y}=\frac{1}{r}\frac{\partial}{\partial r}\left[r\left(\mu+\frac{\mu_t}{\sigma_k}\right)\frac{\partial k}{\partial r}\right]+\frac{\partial}{\partial y}\left[\left(\mu+\frac{\mu_t}{\sigma_k}\right)\frac{\partial k}{\partial y}\right]+P-G-\rho\varepsilon \tag{5}$$

$$\frac{\partial(\rho\varepsilon)}{\partial t}+\frac{1}{r}\frac{\partial(r\rho u\varepsilon)}{\partial r}+\frac{\partial(\rho v\varepsilon)}{\partial y}=\frac{1}{r}\frac{\partial}{\partial r}\left[r\left(\mu+\frac{\mu_t}{\sigma_\varepsilon}\right)\frac{\partial \varepsilon}{\partial r}\right]+\frac{\partial}{\partial y}\left[\left(\mu+\frac{\mu_t}{\sigma_\varepsilon}\right)\frac{\partial \varepsilon}{\partial y}\right]+C_1\frac{\varepsilon}{k}(P+G-C_3G)-\rho_w C_2\frac{\varepsilon^2}{k} \tag{6}$$

where P is the generation of turbulence kinetic energy due to mean velocity gradients, that is, due to shear, and, G, corresponds to the generation of turbulence kinetic energy due to buoyancy [2,6].

$$P = \mu_t \left[2\left(\frac{\partial u}{\partial y}\right)^2 + 2\left(\frac{\partial v}{\partial r}\right)^2 + 2\left(\frac{v}{r}\right)^2 + \left(\frac{\partial u}{\partial r} + \frac{\partial v}{\partial y}\right)^2 \right] \quad (7)$$

$$G = -\left| \beta g \frac{\mu_t}{\rho \sigma_t} \frac{\partial \rho}{\partial y} \right| \quad (8)$$

In Eqs. (5), and (6), σ_k=1.0 and σ_ε=1.3 are the turbulent Prandtl numbers for k and ε, respectively. In Eq. (6), C_1=1.44 and C_2=1.92 are constants. The constant C_3 takes a value of 0.8-1.0 [2,6]. The value of 1.0 is used in the present simulation. In Eq. (8), σ_t=0.85 is the turbulent Prandtl number and β is the volume expansion factor introduced by Choi and Garcia [7]. Unfortunately, there is no explicit range for volume expansion factor in the literature. In the present simulation, the value of β=1.0 is used according to Weiss et al. [6]. For stably stratified flow simulation, μ_t in Eq. (8) is replaced with Eq. (4) and the coefficient of k is taken into the left side of numerical formulation.

2. Conservation of Mass in Turbulent Flows

The sludge transport equation for turbulent flow may be written as [1-4,6]:

$$\frac{\partial(\rho C)}{\partial t} + \frac{1}{r}\frac{\partial(\rho u C)}{\partial r} + \frac{\partial(\rho v C)}{\partial y} = \frac{1}{r}\frac{\partial}{\partial r}\left[r\left(f\mu + \mu_t/\sigma_r\right)\frac{\partial C}{\partial r}\right] + \frac{\partial}{\partial y}\left[\left(f\mu + \mu_t/\sigma_y\right)\frac{\partial C}{\partial y} + V_s C \right] \quad (9)$$

where C is concentration in g/L, V_s=V_s(C) is the settling velocity function and σ_r and σ_y are Schmidt number assumed of 0.7 in r and y direction [6]. Also, f is the plastic diffusion coefficient that is used for model comparison and only takes the values of 0 or 1. As noted by DeClercq [1], using a rheology function with yield stress means a large amount of viscosity in the regions with low shear rates. This means high diffusion in the concentration equation and overestimation of the blanket height. So Lakehal et al. [2] and Wises et al. [6] removed the molecular viscosity from the diffusion coefficient of ther concentration equation. Molecular viscosity in non-Newtonian fluids takes a high value (in some cases more than turbulent viscosity) and is not negligible. Also, there is no considerable change between Newtonian and non-Newtonian fluid results when molecular viscosity is removed from the concentration equations.

In the present simulation, as presented in Eq. (9), an alternative definition of concentration diffusion that includes molecular viscosity is used. The definition is similar to McCorquodale et al.'s [3], but the more common Schmidt number is used instead of a diffusion coefficient.

MIXTURE DENSITY

The equation of state links mixture density, ρ, to the concentration, C, of the suspended sludge [6,8]:

$$\rho = \rho_w + \left(\frac{\rho_s}{\rho_w} - 1\right) C \quad (10)$$

where ρ_w is density of clear water, ρ is local density of the mixture. Dahl (1993) and Nopens (2005) measured the sludge density as a function of the sludge concentration using a pycnometer. They found the values of 1,600 kg/m^3 for the dry sludge density, ρ_s, from a fit of Eq. (10) to their measured data [6,8].

Table 1. Empirical constants used in settling velocity function [6]

Temperature	V_0 (m/h)	r_h (L/g)	r_p (L/g)	C_{min} (g/L)
15 °C	4.3748	0.2501	2.501	5.2×10^{-3}
20 °C	3.1248	0.2355	2.355	5.2×10^{-3}

SETTLING VELOCITY

The settling velocity is expressed by using the double-exponential function of Takacs et al. (1991) [1,2,6], which is given by:

$$V_s = V_0 \left[e^{-r_p(C-C_{min})} - e^{-r_h(C-C_{min})} \right] \quad (11)$$

where V_0 (m/s) is a reference settling velocity, r_h and r_p (L/g) induce the domination of the first and the second term in the equation, for the falling and the rising part, respectively. According to Weiss et al. [6] the value for r_p is generally one order of magnitude larger than that of r_h. The constant C_{min}, is the concentration of non-settleable solids in the effluent of the clarifier. Based on Weiss et al. experiments, required constants are presented in Table 1.

BOUNDARY CONDITIONS

1. Inlet

At the clarifier inlet, the inlet concentration, C_{in}, is applied, which is equal to the concentration at the outlet of the aeration basin, and the inlet velocity, v_{in}, is used. The turbulence kinetic energy at the inlet, k_{in}, is calculated using $k_{in}=1.5\times(I_u v_{in})^2$ where I_u=0.224 is the turbulence intensity [1,2,6]. Dissipation rate at the inlet, ε_{in}, is obtained from blow equation [1,2,6]:

$$\varepsilon_{in} = \frac{C_\mu^{3/4} k_{in}^{3/2}}{\kappa L_u} \quad (12)$$

where κ=0.4 is the von Karman constant. The turbulence length scale, $L_u=0.5\times R_b$, where R_b is the radius of the baffle skirt in the inlet region of the clarifier [2,6].

2. Free Surface

The vertical movement of the free surface of the clarifier is assumed to be negligibly small. This assumption simplifies the computation greatly, as it helps to keep the computational effort to a minimum. The vertical (axial) velocity component is thus set to zero at the surface, v=0, and the horizontal (radial) velocity component, u, is computed assuming full slip, that is, the surface is treated as a stress-free entity.

3. Outlet

At the effluent outlet boundary, the values of the variables are extrapolated from computed near-outlet values. This extrapolation sets the stream-wise gradients to zero.

4. Wall

The no-slip condition must be obeyed at all solid boundaries, that is, u, v=0 at all clarifier walls. The boundary condition of concentration is that zero gradients perpendicular to all solid walls, so that the solid walls are made impenetrable for the scalar species. Also settling velocity is set to zero at horizontal walls. Logarithmic wall function (Eq. (13)) is applied to model the turbulent flow in the

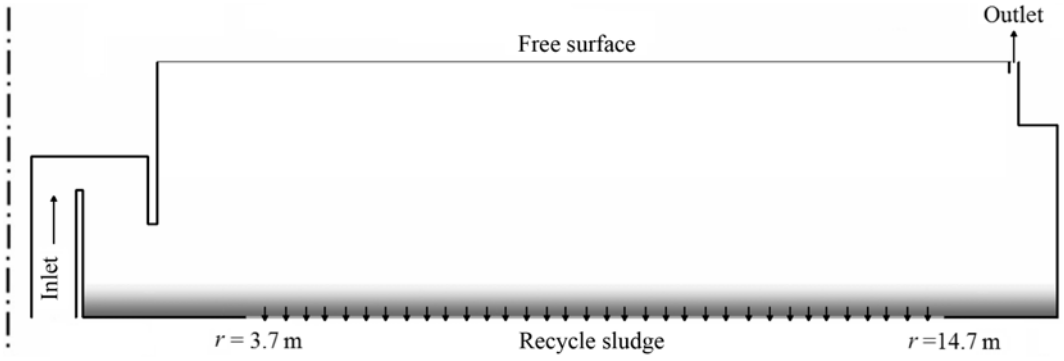

Fig. 2. Special boundary condition assumed for recycled sludge outlet.

near-wall region of the clarifier [9]:

$$u^+ = \begin{cases} y^+ < 5 & y^+ \\ -3.05 + 5\ln y^+ & 5 < y^+ < 30 \\ 5.5 + 2.44\ln y^+ & y^+ > 30 \end{cases} \quad (13)$$

where $u^+=u/(\tau_w/r)^{1/2}$ is the shear velocity of the first grid from the wall, $y^+=\rho y(\tau_w/r)^{1/2}/\mu$ is the non-dimensional physical distance of the first grid from the wall, and τ_w is the wall shear stress [10].

5. Sludge Outlet

Using the first withdrawing method, as shown in Fig. 2, sludge is removed from the bottom of clarifier at the pipes zone from r= 3.7 m to r=14.7 m. Flow is sucked from the bottom with uniform mass flow rate. Flow rate is divided to all computational cells and corresponding suction velocity is calculated. Radial velocity is assumed to be zero at this boundary. Boundary condition on the concentration is that the gradients perpendicular to bottom are set to zero. Flow is sucked with low velocity in order of 10^{-4} m/s which is two orders of magnitude lower that the input velocity, so logarithmic wall function is applied to model the turbulent flow in the near-wall region of the clarifier.

RHEOLOGY OF ACTIVATED SLUDGE

The definition of shear stress is used for calculation the viscosity of activated sludge:

$$\mu_p = \frac{\tau_{ry}}{\dot{\gamma}} \quad (14)$$

where μ_p is the plastic viscosity that should be replaced with molecular viscosity in all equations, τ_{ry} is the shear stress of flow with individual definition in each model, and $\dot{\gamma}$ is the shear rate. According to Vradis and Protopapas [11], the shear rate may be defined as:

$$\dot{\gamma} = \sqrt{2\left(\frac{\partial u}{\partial y}\right)^2 + 2\left(\frac{\partial v}{\partial r}\right)^2 + 2\left(\frac{v}{r}\right)^2 + \left(\frac{\partial u}{\partial r} + \frac{\partial v}{\partial y}\right)^2} \quad (15)$$

Bingham plastic, Herschel-Bulkley (pseudo plastic with yield stress), pseudo plastic and dilatant models may be defined for behavior of non-Newtonian fluids [1]. Behn (1960) classified sewage sludges as Bingham fluids. Sozanski et al. (1997) also applied this type of model for thickened sludge. Others employed both Bingham and pseudo plastic models [12,13], while Manoliadis and Bishop (1984) only applied the pseudo plastic model. Different models have been compared by Sanin [14] and for this type of sludge the pseudo plastic model appeared to fit the best [1,12-14].

Another class of non-Newtonian fluids, the dilatant fluids, exhibits a behavior which is opposite to that of the pseudo plastic fluids. According to Behn (1960), this flow type does not appear in wastewater treatment [1]. A pseudo plastic flow with yield stress is called Herschel-Bulkley fluid. In this respect, Monteiro (1997) performed a comparison between this and the Bingham model. A better fit with the Herschel-Bulkley model was obtained by DeClercq [1].

Although all mentioned models have been successfully fitted with the rheological data, the appropriate model largely depends on the sludge properties. Other parameters such as the specific floc surface have been investigated by Dymaczewski et al. (1997), but the solids concentration appears to be the most important variable related to viscosity [1,2,6].

1. Standard Casson Model

The relationship between shear stress and shear rate follows the Casson law for the shear rates lower than 50 s^{-1} [6,8]. The Casson equation for the sludge viscosity can be expressed as [6,8]:

$$\tau_{ry}^{1/2} = K_1 + K_2\dot{\gamma}^{1/2} \quad (16)$$

where $\dot{\gamma}$ is the shear rate, K_1 is the Casson yield stress parameter, and K_2 is the Casson viscosity parameter. Rheology experiments of Weiss et al. [8] show that K_1 depends quadratically on the concentration:

$$K_1 = AC^2 + BC \quad (17)$$

where A, and B are constant. According to Weiss et al. [8], the viscosity parameter, K_2, does not show a clear dependence on concentration and appears to be independent of concentration over the range of concentrations studied. Neglecting the yield stress parameter, K_1, Dollet (2000) found that K_2 does not depend on the sludge concentration, and gave a mean value of 0.032 $kg^{1/2}$ $m^{-1/2}$ $s^{-1/2}$ for the Casson viscosity parameter [6,8]. Dollet's observation on the concentration dependence of K_2 and its mean value demonstrates a good correspondence with Weiss et al. [6,8]. Weiss et al. [6,8] assumed that K_2 is independent of the concentration for $C \geq C^*$=2 g/L and equal to the mean value, $K_{2,ave}$. For the water viscosity value, μ_w, to emerge correctly as $C \rightarrow 0$, K_2 is assumed to depend linearly on the concentration on the interval $0 \leq C < C^*$. Thus, for $C \geq C^*$:

Table 2. Constants of Casson fluid model [6]

Temperature	A ($m^{11/2}kg^{-3/2}s^{-1}$)	B ($m^{5/2}kg^{-1/2}s^{-1}$)	$K_{2,ave}$ ($kg^{1/2}m^{-1/2}s^{-1/2}$)	μ_w (Pa·s)
15 °C	0.00281	0.0176	0.0445	1.163×10^{-3}
20 °C	0.00319	0.0146	0.0436	1.303×10^{-3}

$$K_2=K_{2,ave} \tag{18}$$

and for 0≤C<C*:

$$K_2=\mu_w^{1/2}+\left(\frac{\overline{K}_2-\mu_w^{1/2}}{C^*}\right)C \tag{19}$$

Based on Weiss et al. [6] experiments, the values of required constants for two different temperatures are presented in Table 2.

2. Modified Casson Model

Plastic viscosity using Casson model can be defined as:

$$\mu_p=(K_1/\dot{\gamma}^{1/2}+K_2)^2 \tag{20}$$

Shear stress - shear rate charts of the Casson model in various concentrations are presented in Figs. 3, and 4. Results show that there is good agreement between the Casson model and data provided by Weiss et al. [8]. Using Eq. (20), the Casson model gives high values of plastic viscosity at very low shear rates. In the present simulation, plastic viscosity is not neglected in concentration diffu-

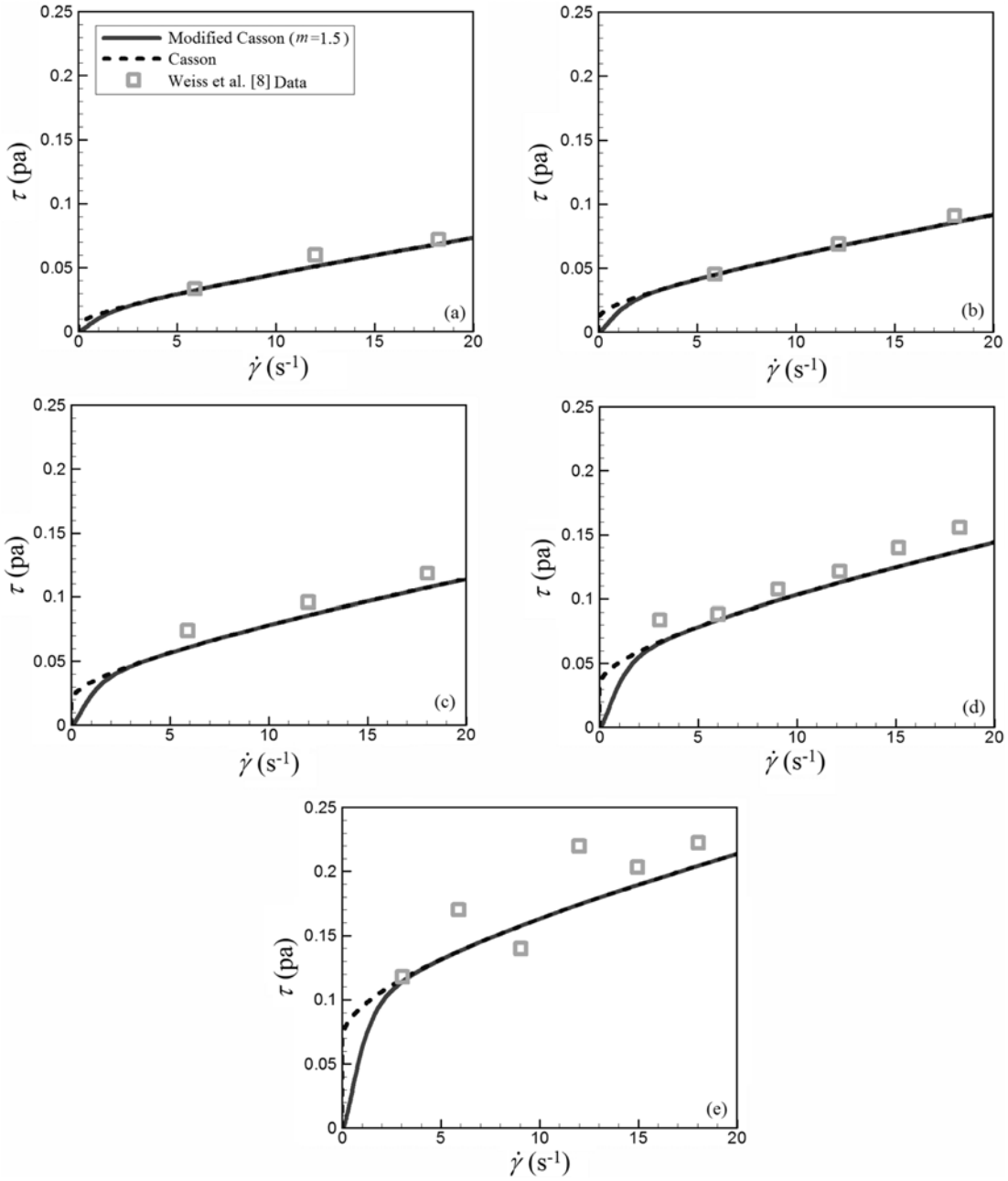

Fig. 3. Shear stress versus shear rate for modified and standard Casson models at T=15 °C. (a) C=2.82 g/L, (b) C=3.71 g/L, (c) C=4.56 g/L, (d) C=5.48 g/L. (e), C=7.04 g/L.

sion equation. Using the Casson model leads to overestimation of blanket height due to high concentration diffusion. To overcome this problem the Casson model is modified by using an exponential term. Similar exponential term was also used by DeClercq [1] using modified Herschel-Bulkley model. The modified Casson fluid model used in this simulation is defined as below:

$$\mu_p = \{[1-\exp(-m\dot{\gamma})]K_1/\dot{\gamma}^{1/2} + K_2\}^2 \quad (21)$$

where m is the shear rate growth factor. Using this formulation, high viscosities at low shear rates are modified. Using low and high values of shear rate growth factor, more and less modification of viscosity is achieved. The minimum range of shear rate growth factor, m, can be found by the low shear rate experimental data. On the other hand, model curve fitting should also be applicable using a modified Casson model.

Shear rate growth factor, m, of the modified Casson model should be determined by using experimental results at low shear rates that are not available. Fortunately, this factor determines the blanket height of activated sludge. Using a trial and solution procedure, the values of shear rate growth factors can be determined. After several trials and solutions, shear rate growth factors are calculated as m=1.5, and m=2.3 for temperature of 15 °C and 20 °C, respectively. Modi-

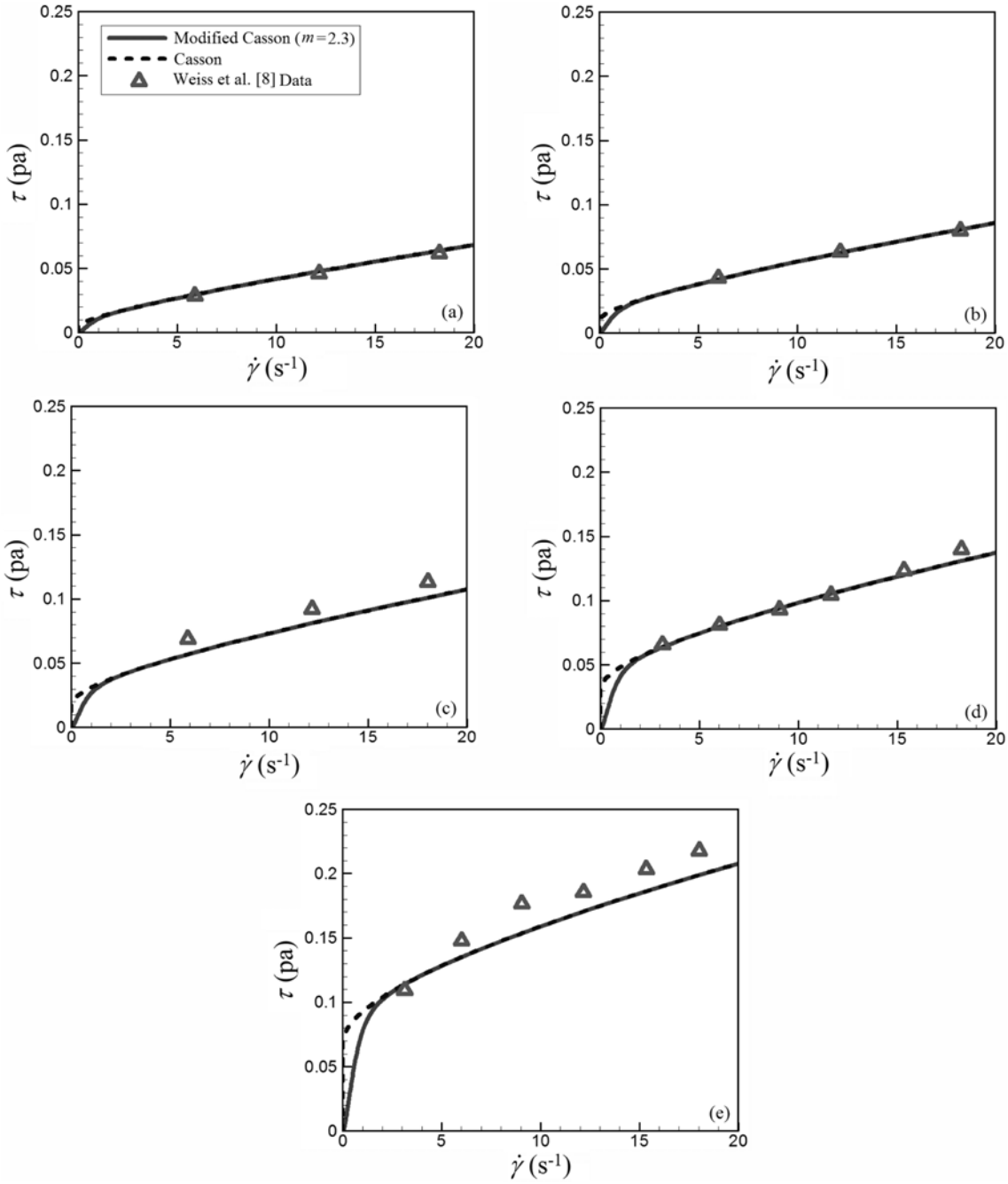

Fig. 4. Shear stress versus shear rate for modified and standard Casson models at T=20 °C. (a) C=2.82 g/L, (b) C=3.71 g/L, (c) C=4.56 g/L, (d) C=5.48 g/L. (e), C=7.04 g/L.

fied Casson model is shown in Figs. 3 and 4 for T=15 ºC and T= 20 ºC, respectively. These figures show that introduced Casson model excellently fitted the experimental data.

NUMERICAL SOLUTION AND RESULTS

A finite volume Staggered SIMPLEC (Semi implicit method for pressure linked equations-corrected) code provided using Intel Visual Fortran. Time step of Δt=0.5 s is used. Convergence was attained after about 40,000 s. Simulations are based on two clarified loads presented in Table 3. Experiments were carried out by Weiss et al. [6] at March and July 2005 with temperature of 15 ºC and 20 ºC, respectively. Clarifier load is low and high in March and July, respectively.

1. Mesh Sensitivity Analysis

Three grid dimensions that are shown in Fig. 5 are used for mesh sensitivity analysis: 200×99, 350×150, and 500×200. The grid independency is checked and illustrated in Fig. 6. This figure depicts the concentration profile at r=11.0 m and low clarifier load, and at r=13.5 m and high clarifier load for various grid sizes. Results show that there is no benefit in using a grid dimension more than 350×150, so a grid dimension of 350×150 is appropriate. This grid independency is also checked at other radiuses that are not brought

Table 3. Clarifier load specification [6]

Clarifier load	Low load March (T=15 ºC)	High load July (T=20 ºC)
Input concentration	3.91 g/L	4.93 g/L
Input velocity	4.9 cm/s	6.5 cm/s
Recycled mass flow rate	75.7 kg/s	100.4 kg/s

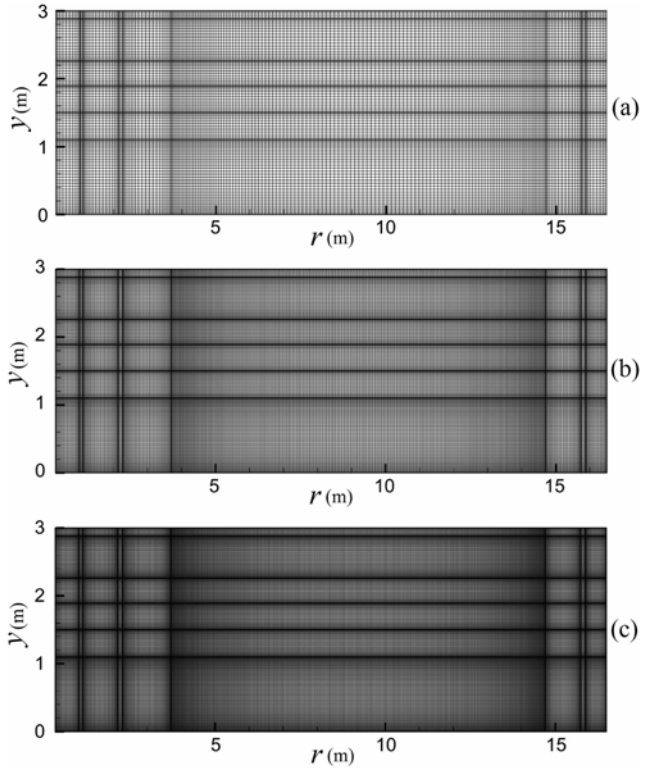

Fig. 5. Grid dimensions used for mesh sensitivity analysis: (a) 200 ×99 (b) 350×150, and (c) 500×200.

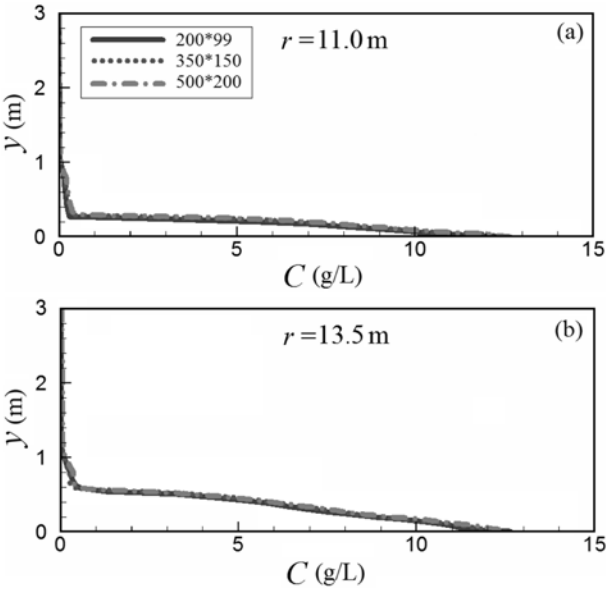

Fig. 6. Mesh sensitivity analysis at: (a) r=11.0 m and low clarifier load, (b) r=13.5 m and high clarifier load.

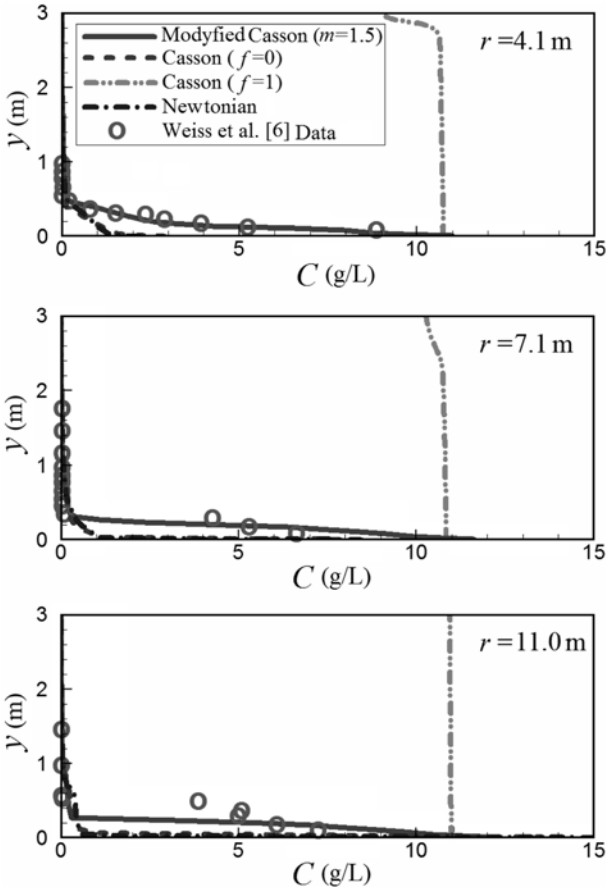

Fig. 7. Concentration profiles at various radiuses: Low clarifier load (March).

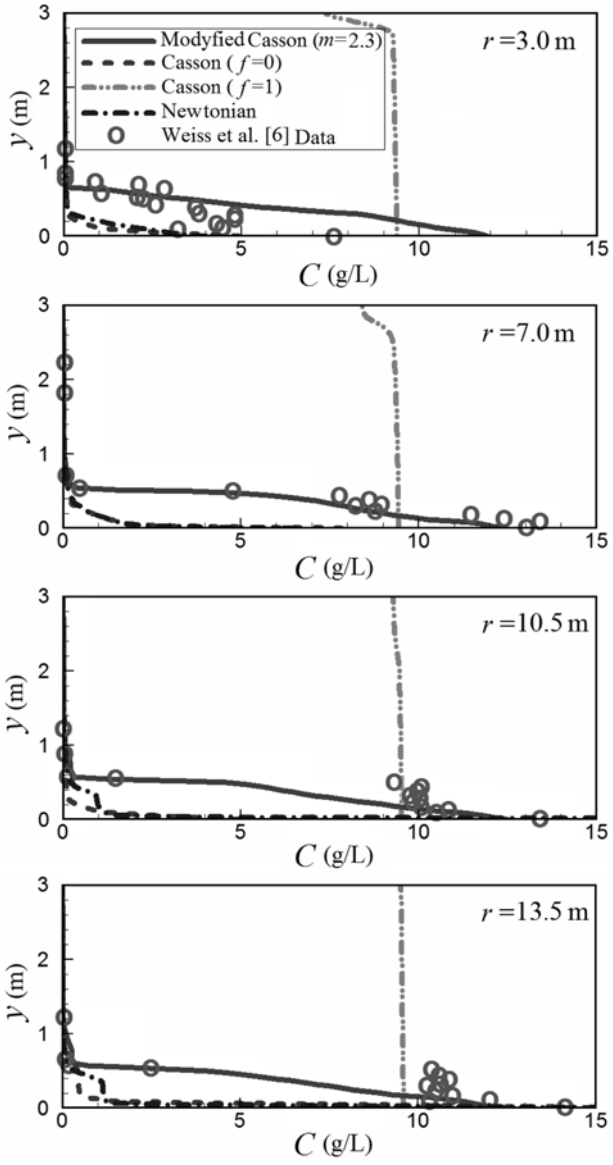

Fig. 8. Concentration profiles at various radiuses: high clarifier load (July).

here.

2. Standard and Modified Casson Model

Concentration and velocity profiles in various distances from the center line are presented in Figs. 7 and 8. Numerical simulations are done using four models:

1- Modified Casson model (f=1).
2- Casson model (f=1).
3- Casson model neglecting plastic viscosity in concentration diffusion term (f=0).
4- Newtonian model.

Fig. 7 shows the concentration profile in low clarifier load. The Casson model estimates all clarifier zones as activated sludge, and consequently causes high concentration diffusion and overestimation prediction. Third Casson model neglects plastic viscosity in concentration diffusion term (f=0), and therefore dose not have any agreement with the experimental data. This shows that plastic viscosity in concentration diffusion term is not negligible. Close agreement between the Newtonian model and this model is observed. The present simulation that is based on modified Casson model is well correlated with the experimental data of Weiss et al. [6]. High clarifier load concentration profiles are depicted in Fig. 8. The similar trend of Fig. 7 is observed.

Total agreement between calculated concentration profiles and Weiss et al. data is good. Small differences can be found at r=11 m in March and at r=3 m in July. Small deviance at r=11 m in March is underestimation of blanket height and overestimation of concentration. While, small deviance at r=3 m in July is only concentration overestimation.

Depending on the radial distance from the center of the clarifier, the concentration profiles show that the sludge blanket height has a value of 30-45 cm in March, and 65-75 cm in July. For blanket height calculation, small blanket height overestimation at low concentration in some cases (a bump in the outset of profiles at r=11 m at March, r=10.5 m, and r=13.5 m at July) is neglected. The sludge blanket is more elevated at shorter distances from the clarifier center in both sets of clarifier loads. The sludge concentration at the clarifier bottom in all cases is about 12 g/L. But in March, i.e., low load clarifier, the maximum bottom concentration is located in a very thin layer at the bottom.

The radial velocity profiles for two load scenarios are presented

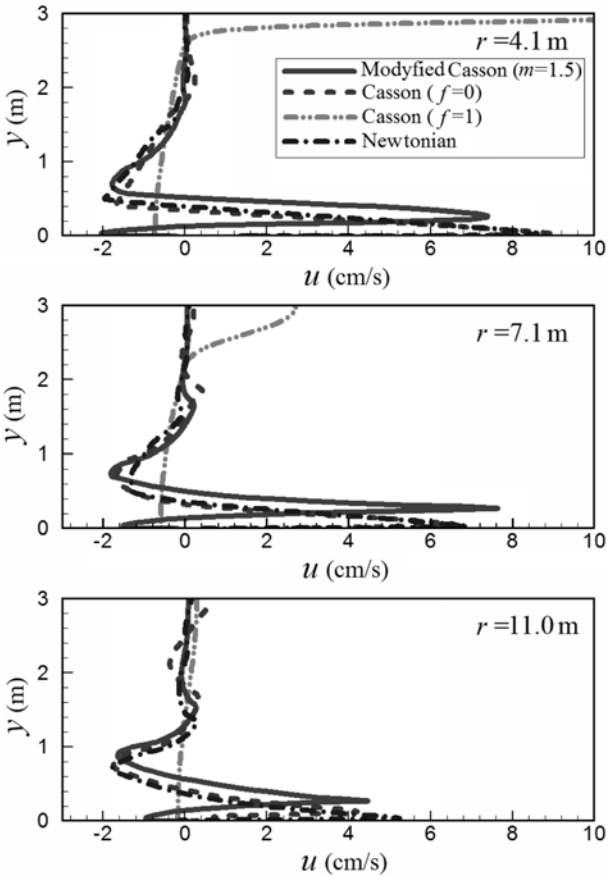

Fig. 9. Velocity profiles at various radiuses: low clarifier load (March).

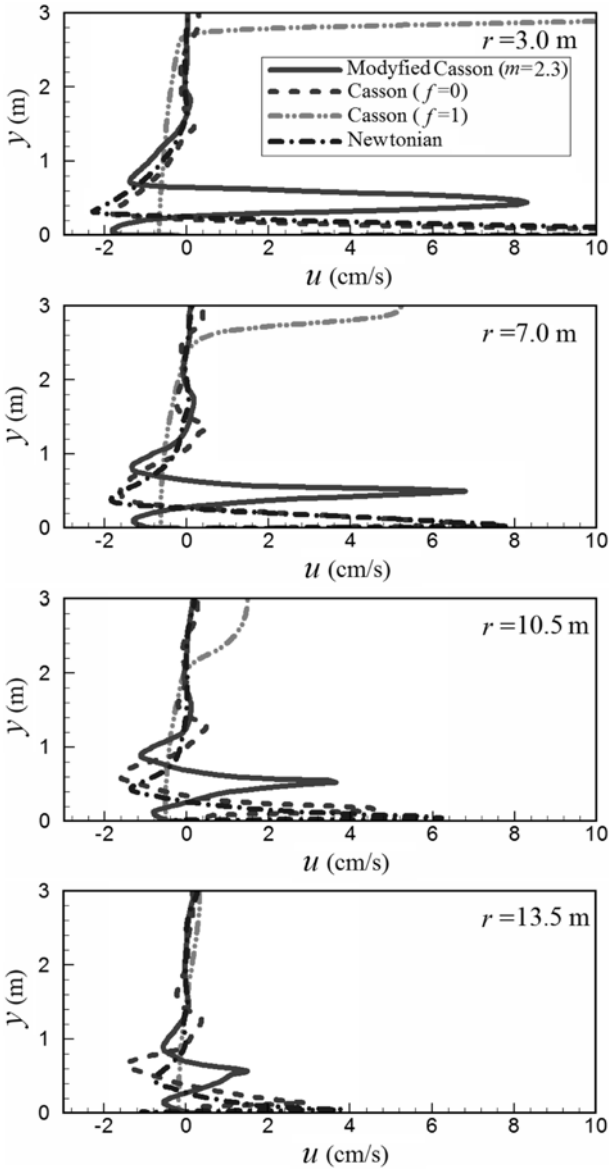

Fig. 10. Velocity profiles at various radiuses: high clarifier load (July).

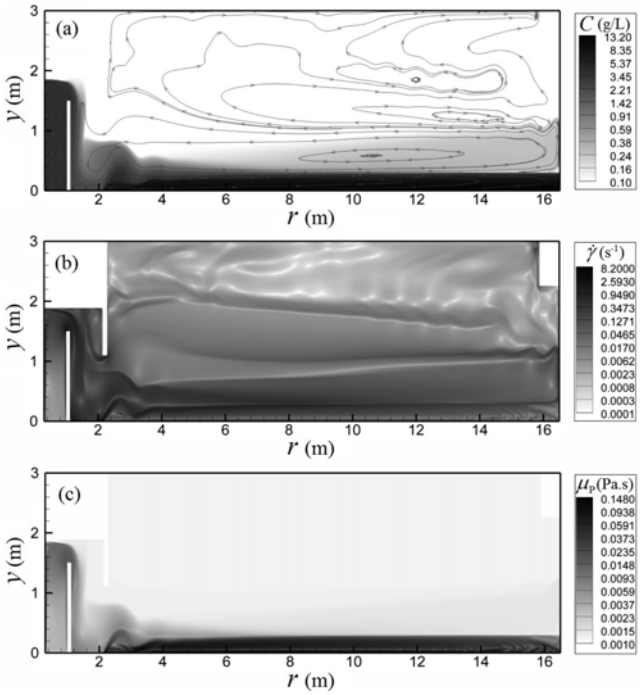

Fig. 11. (a) Concentration counters and flow streamlines, (b) shear rate, and (c) plastic viscosity: low clarifier load (March).

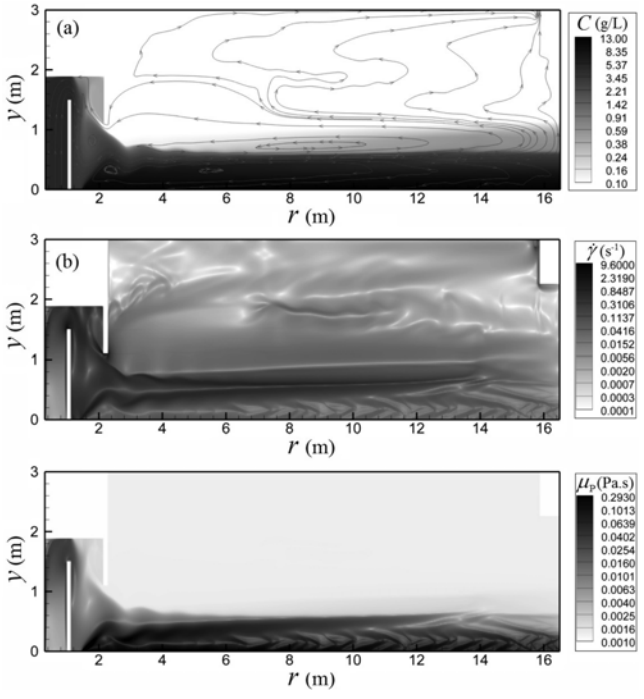

Fig. 12. (a) Concentration counters and flow streamlines, (b) shear rate, and (c) plastic viscosity: high clarifier load (July).

in Figs. 9 and 10. The maximum velocity is at the upper side of the blanket height. Also, two backward velocity zones are found above and below the maximum velocity. These negative velocities are corresponding to zones of flow reversal and recirculation in the clear water region and in the near-bottom region. Casson model using f=0 and also Newtonian models have similar predictions, but due to lower blanket height prediction, the maximum velocity shifts downward. The Casson model using f=1 predicts the maximum velocity at free surface that only could be acceptable when the clarifier is filled by sludge.

Flow streamline, concentration counters, plastic viscosity, and shear rate of the modified Casson model are presented in Fig. 11 for March clarifier load. Streamlines show that the flow field is complex with several recirculation zones. The main recirculation is right above the sludge blanket. Also, another main recirculation can be found in the sludge blanket. The maximum concentration is calculated as 13.2 g/L. Shear rate changes between 2.2×10^{-5} and 8.2 s^{-1}. The highest shear rates are encountered in two regions:

1. In the inlet region, where the incoming stream of activated sludge is bounded by the walls and baffles.
2. Around the upper limit of the sludge blanket, close to the clarifier inlet.

The shear rate in activated sludge region is high due to recirculation in activated sludge that is bounded with a wall and another recirculation above it. The minimum level of shear rate is 2.2×10^{-5} i.e., too low. This occurs in the clear water zone due to relatively still flow. Small shear rates lead to high plastic viscosity. Fortunately, low shear rates occur in the clear water zone that concentration is small. Fig. 11(c) shows how the viscosity of the activated sludge is defined. Plastic viscosity is proportional to shear rate inversely, so at low shear rates, the value of plastic viscosity is high. Comparing Figs. 11(b) and 11(c), completely similar zone can be found in the activated sludge zone. At clear water zone above the activated sludge, low shear rate also tends to increase viscosity. Plastic viscosity is proportional to concentration directly, so this correlation corrects plastic viscosity in the clear water zone. Plastic viscosity changes between 0.001 and 0.148 Pa·s in this case.

Similar condition can be found in Fig. 12 for July clarifier load.

Table 4. Sink terms used in governing equations using 3rd withdrawing method [6]

Equation	Sink term
Continuity	q_{rec}/V_{rec}
Momentum in r direction	$q_{rec}u/V_{rec}$
Momentum in y direction	$q_{rec}v/V_{rec}$
Turbulent kinetic energy	$q_{rec}k/V_{rec}$
Rate of dissipation of turbulence	$q_{rec}\varepsilon/V_{rec}$
Concentration	$q_{rec}C/V_{rec}$

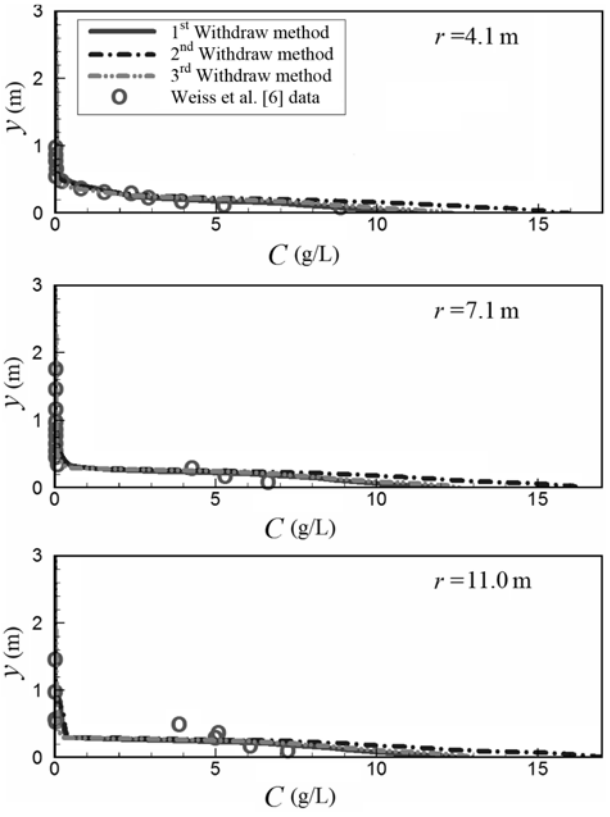

Fig. 13. Concentration profiles of various withdrawing methods: low clarifier load (March).

Here the sludge blanket height is more than March. The maximum concentration is 13.0 g/L. Two main recirculation zones also can be found in the activated sludge zone and right above it. In this case shear rate changes between 6.8×10^{-6} and 9.6 s^{-1} and plastic viscosity changes between 0.001 and 0.293 Pa·s.

ALTERNATIVE SLUDGE WITHDRAWING METHODS

Two alternative withdrawing methods are used for sludge withdrawing sensitivity analysis. 1st withdrawing method was explained before.

2nd withdrawing Method: Sludge is removed from circular shift of pipes' position at the bottom boundary: According to Weiss et al. [6] the pipes' diameter should be about 48cm. Also, six used pipes should be positioned in the range of r=3.7 m to r=14.7 m. Therefore, the position of pipes is assumed at r=4.61 m, r=6.45 m, r=8.29 m, r=10.13 m, r=11.97 m, and r=13.81 m.

3rd withdrawing Method: Sludge is removed using sink term in

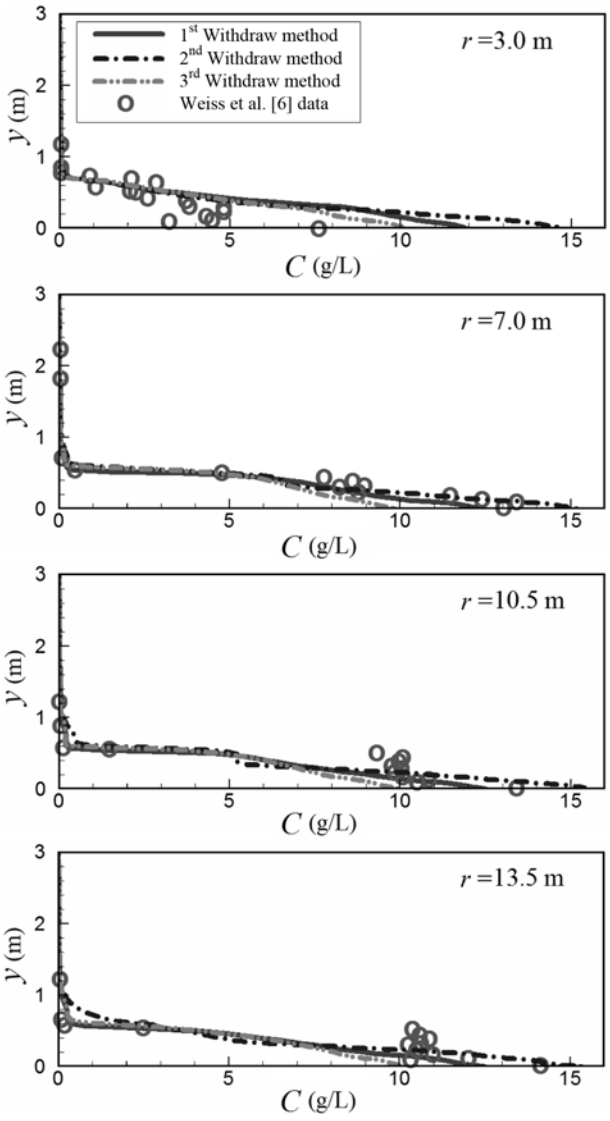

Fig. 14. Concentration profiles of various withdrawing methods: high clarifier load (July).

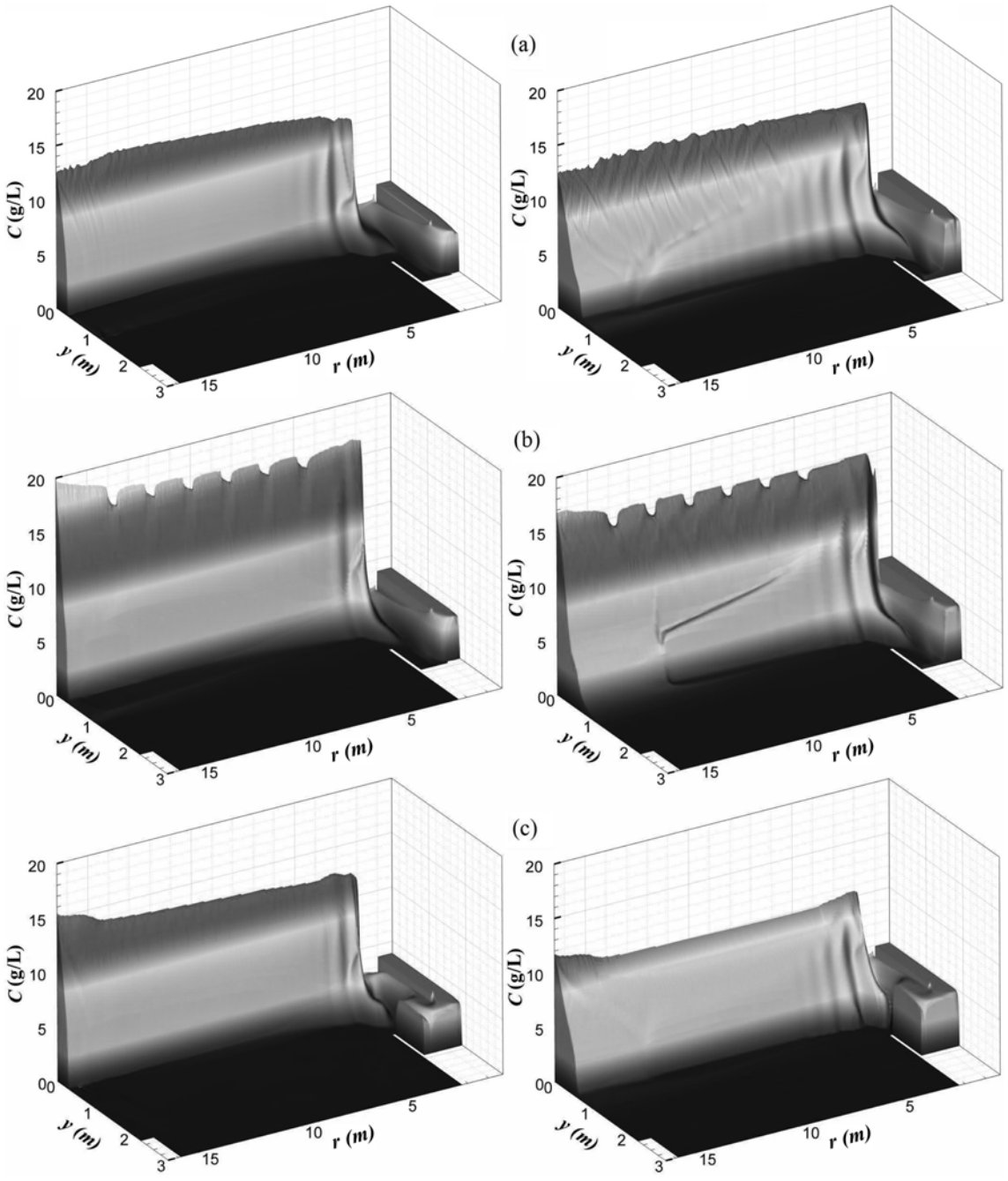

Fig. 15. (a) Concentration distribution using (a) 1st, (b) 2nd, and (c) 3rd withdrawing methods. Left: low clarified load, Right: high clarifier load.

governing equations: According to Weiss et al. [6] the pipes' entrance is at the height of 0.15 m above the bottom boundary. Sink terms presented in Table 4 are added to governing equations in the range of r=3.7 m to r=14.7 m and y=0 to y=0.15 m.

In Table 4, q_{rec} is the recycled mass flow rate and V_{rec} is the volume of the sludge removal zone. Concentration and profiles of three withdrawing methods are presented in Figs. 13, and 14 for low and high clarifier loads. Also, concentration distribution is presented in Fig. 15.

Using 2nd sludge withdrawing method, and removing the sludge from the pipes position, leads to high withdraw at these positions, so the concentration decreases at pipes position and increases at other regions as shown in Fig. 15(b). Also, settled sludge at the position where there is no pipe at the bottom boundary cannot be removed correctly. This leads to more concentration prediction, and as shown in Fig. 15(b), the concentration in this case is more than 1st withdrawing method. The maximum concentration in this case is 19.7 g/L and 16.8 g/L for low and high clarifier load, respectively. The ratio of recycle sludge mass flow rate to inflow mass flow rate is 0.54 for both clarifier loads. As the settled concentration is about 4 times more than input concentration, the effect of input velocity is more than input concentration. This may be the cause of more concentration prediction at March.

Concentration profiles presented in Figs. 13 and 14 are not at the pipes position, and more concentration than 1st sludge withdrawing method is predicted. The sludge concentration at the clarifier bottom is about 3 g/L more than 1st withdrawing method at March, which is about 2 g/L more than 1st withdraw method at July. More concentration means more concentration difference between clear water and activated sludge zones, so the value of shear rate growth factor, m, should be decreased to prevent overestimation prediction. After several trials and solutions, the values of 0.5 and 1.1 are found for temperatures of 15 and 20 °C, respectively. Using these values, the difference of results with 1st withdraw method is only more concentration prediction at the clarifier bottom that does not match with experimental data. Also, from using low values of shear rate growth factor, more deviation to shear stress-shear rate data fitting occurred, so this withdraw method is not acceptable.

Using 3rd sludge withdrawing method and removing the sludge using sink term in governing equations leads to less concentration estimation than two other methods at July, so more shear rate growth factor is needed due to less concentration difference between clear water and sludge blanket. After several trials and solutions the values of 1.3 and 4.0 were estimated for temperatures of 15 and 20 °C, respectively. The value of July is more than 1st withdrawing method and model data fitting are also applicable using this value. Concentration profiles presented in Fig. 14, show that 3rd withdraw method underestimates the bottom concentration about 4 g/L at high clarifier load. It should be noted that the value of concentration cannot be changed by shear rate growth factor effectively, and this factor can only change the height of the sludge blanket.

To investigate which withdrawing method is appropriate, errors based on input concentration are presented in Table 5. The error is defined as the average differences between measured and predicted concentrations at specified heights. This table shows the average error of 32.7% for 1st withdrawing method and the 36.9% for 3rd withdrawing method, so the experimental data are closer to the 1st

Table 5. Percentage errors of three withdraw methods

Clarifier load	Low	High	Average
1st Withdrawing method	22.9%	42.4%	32.7%
2nd Withdrawing method	38.4%	44.4%	41.4%
3rd Withdrawing method	27.1%	46.8%	36.9%

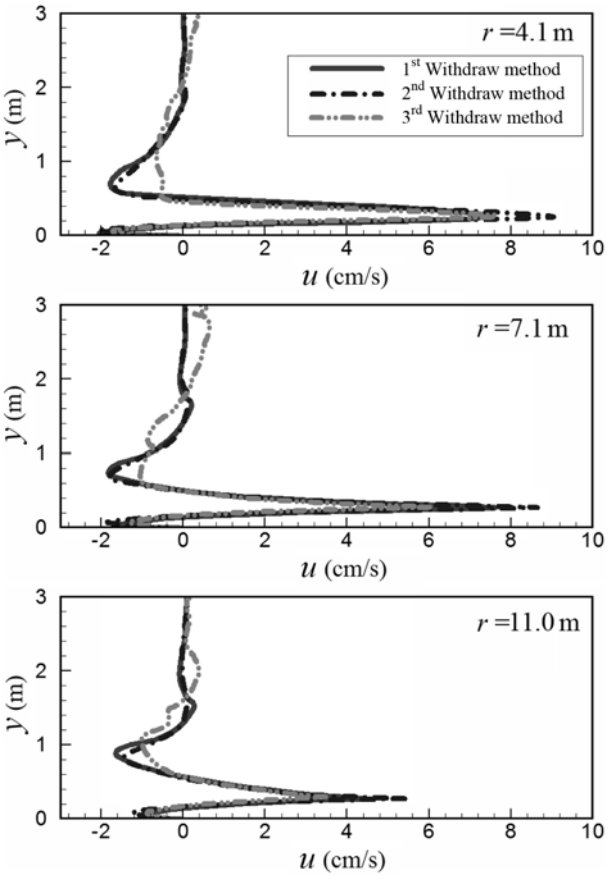

Fig. 16. Velocity profiles of various withdraw methods: low clarifier load (March).

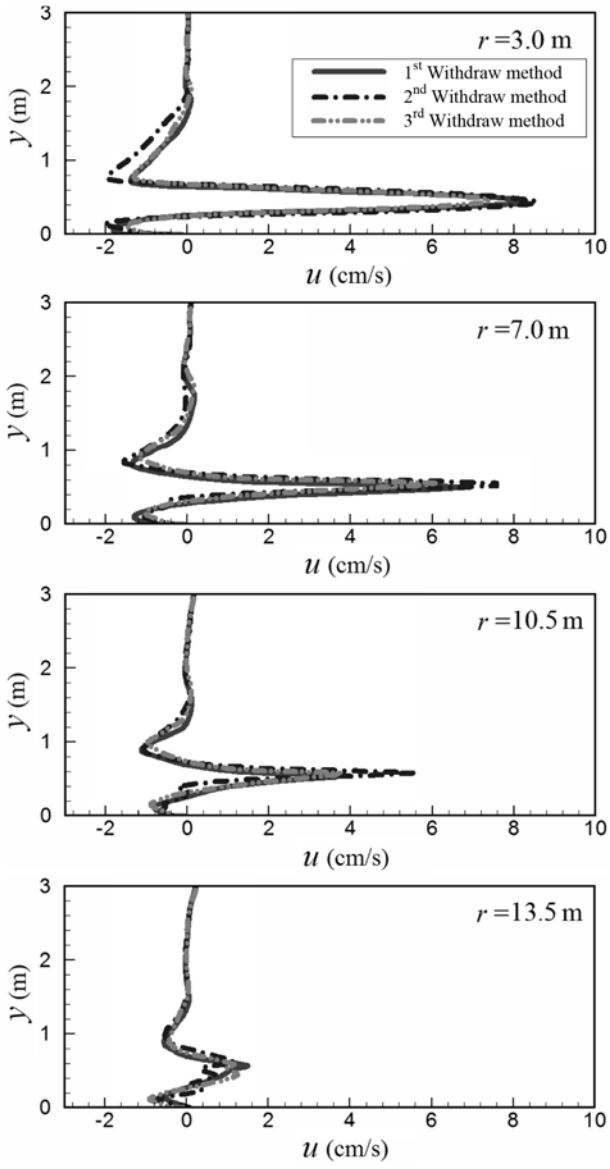

Fig. 17. Velocity profiles of various withdraw methods: high clarifier load (July).

withdrawing method. This shows that the average error of 41.4% for the 2nd withdraw method that is more than the other two methods. Therefore, 1st withdrawing method is the best choice for 2-D simulation of slowly rotating pipes.

Velocity profiles of three withdrawing methods are presented in Figs. 16 and 17. The sludge blanket height is from experimental data using the shear rate growth factor. The peak velocity of the three models occurred at the same zones. The value of peak velocity changed with the concentration. Changing the concentration at the bottom is the cause of changing the peak velocity, especially at the outset of clarifier. Heavy fluid moves at the lower height. This may be the cause of increasing the maximum velocity at high concentration that is right above the sludge blanket zone.

CONCLUSION

Numerical simulation of a secondary clarifier with activated sludge and suction lift removal system is performed. First, a suction lift removal system is simulated by activated sludge withdrawing at the bottom of the clarifier. Standard Casson fluid model presented by of Weiss et al. [6] is converted to a modified Casson model. The cause of this conversion is extra high viscosity simulated by the Casson model at low shear rates. Plastic viscosity in the concentration diffusion equation is not neglected, and so high plastic viscosity calculated by Casson model leads to high concentration diffusion and overestimation of blanket height. To overcome this problem, an exponential term is added to the Casson yield stress. Therefore, plastic viscosity is decreased at low shear rates. Results show that using this formulation has an agreement compared to experimental data provided by Weiss et al. [6].

Results of the Casson model with concentration diffusion factor, f=0 and 1 and results of Newtonian fluid model are presented. Comparison of results shows that the Casson model using f=0, has no agreement with experimental data and results are close to the Newtonian model. This shows that the plastic viscosity in the concentration equation is not negligible. Also, results of the Casson model using f=1 overestimate the blanket height and give invalid results.

The results of velocity profiles show that the maximum velocity is at the upper sides of activated sludge zones. The maximum velocity in the Casson model using f=1 and non-Newtonian model shifted downward and results are close to each other. Also, the velocity profile of the Casson model using f=0 can be valid when the clarifier is filled with activated sludge.

Concentration counters, flow streamlines, shear rate, and plastic viscosity are illustrated. Results show how concentration and shear rate affect the plastic viscosity. Plastic viscosity is proportional to the inverse of shear rate and directly proportional to the concentration, so low concentration modifies the plastic viscosity at clear water zone.

Two alternative sludge withdrawing methods are used for withdrawing sensitivity analysis. These methods give various sludge blanket heights due to various concentration predictions. The precision values of shear rate growth factors are unknown due to lack of experimental shear stress at low shear rates. So various values of shear rate growth factors are used and the height of the sludge blankets comes from experimental data. Results show that 2nd withdrawing method and removing the sludge from the pipe position is not acceptable due to high concentration prediction and also low shear rate growth factor required. However, sludge is sucked from the pipes position due to 2-D modeling. The pipes in real clarifier are rotating and large amount of sludge is sucked by the pipes suddenly. The measurements of the concentration are done in the other side of slowly rotating pipes, so the effects of suction cannot help us for better results, and uniform flow withdrawing at the bottom of clarifier is closer to real clarifier. Also, results of the 3rd withdraw method show that using sink term in governing equation introduced by Weiss et al [6] cannot correctly simulate the concentration at high clarifier load, and 1st withdrawing method is closer to a real clarifier. The cause may be the change of flow field behavior using sink terms in the governing equation. Therefore, using the 1st withdrawing method and the corresponding values of shear rate growth factors is appropriate.

REFERENCES

1. B. DeClercq, *Computational fluid dynamics of settling tanks: Development of experiments and rheological, settling and scraper sub models*, Ph.D. Thesis, University of Ghent (2003).
2. D. Lakehal, P. Krebs, J. Krijgsman and W. Rodi, *J. Hydraulic Eng.*, **125**, 253 (1999).
3. J. A. McCorquodale, E. J. La Motta, A. Griborio, D. Holmes and I. Georgiou, *Development of software for modeling activated sludge clarifier systems*, A Technology Transfer Report, Department of Civil and Environmental Engineering, University of New Orleans, LA 70148 (2004).
4. L. Szalai, P. Krebs and W. Rodi, *J. Hydraulic Eng.*, **120**, 4 (1994).
5. A. Deininger, E. Holthausen and P. A. Wilderer, *J. Water Res.*, **32**, 2951 (1998).
6. M. Weiss, B. Plósz, K. Essemiani and J. Meinhold, *J. Chem. Eng.*, **132**, 1 (2007).
7. S. C. Choi and M. Garcia, *J. Hydraulic Eng.*, **128**, 55 (2002).
8. M. Weiss, B. Gy. Plósz, K. Essemiani and J. Meinhold, *Sedimentation of activated sludge in secondary clarifiers*, 5th World Congress of Particle Technology (WCPT), Orlando, Florida, US (2006).
9. S. Thangam and C. G. Speziale, *AIAA J.*, **30**, 1314 (1992).
10. W. Rodi, *Calculation of stably stratified shear-layer flow with a buoyancy extended k-ε model*, Turbulence and diffusion in stable environment, J. C. R.Hunt, Ed., Oxford University Press, Oxford, England (1985).
11. G. C. Vradis and A. L. Protopapas, *J. Hydraulic Eng.*, **119**, 95 (1993).
12. P. Battistoni, *Pre-Treatment, Wat. Sci. Tech.*, **36**, 33 (1997).
13. V. Lotito, L. Spinosa, G. Mininni and R. Antonacci, *Wat. Sci. Tech.*, **36**, 79 (1997).
14. F. D. Sanin, *Water SA*, **28**, 207 (2002).